CHARACTERIZATION OF CEMENT KILN DUST FROM BULGARIAN CEMENT PLANTS

Aleksandar Nikolov, Vladislav Kostov-Kytin, Mihail Tarassov, Liliya Tsvetanova, Nicolai B Jordanov, Emilia Karamanova, Ivan Rostovsky

CHARACTERIZATION OF CEMENT KILN DUST FROM BULGARIAN CEMENT PLANTS

Aleksandar Nikolov[1], Vladislav Kostov-Kytin[1], Mihail Tarassov[1], Liliya Tsvetanova[1], Nicolai B. Jordanov[2], Emilia Karamanova[2], Ivan Rostovsky[3]

[1]*Institute of Mineralogy and Crystallography*
Bulgarian Academy of Sciences, Acad. G. Bonchev St.,
Bl. 107, Sofia 1113, Bulgaria, y8sashko@yahoo.com (A.N.);
vkytin@abv.bg (V.K.) ; mptarassov@gmail.com (M.T.);
lilicvetanova79@abv.bg (L.T.).
[2]*Institute for Physical Chemistry, Bulgarian Academy of Sciences*
IPC-BAS, Bl. 11, Acad. G. Bonchev St., Sofia 1113,
Bulgaria, njordanov@ipc.bas.bg (N.J.) ; ekarama@ipc.bas.bg (E.K.).
[3]*Department of Building Materials and Insulations*
Faculty of Civil Engineering,
University of Architecture Civil Engineering and Geodesy,
1 "Hristo Smirnenski" Blvd., Sofia, Bulgaria, i_rostovsky@abv.bg (I.R.).

Received 06 October 2024
Accepted 18 February 2025 *DOI: 10.59957/jctm.v60.i3.2025.11*

ABSTRACT

The cement production is accompanied by generation of fine dust, known as cement kiln dust (CKD), formed during the high-temperature processing of raw materials in the rotary kilns. This study focusses on characterizing CKD from Bulgarian cement plants and explore its physical and chemical properties. The study includes analysing CKD samples from three local cement plants using techniques such as laser diffraction, XRD, XRF, FT-IR, and SEM. Variations have been observed in their physical, chemical, and mineralogical properties likely due to differences in raw materials, kiln conditions and the use of alternative fuels. This research provides valuable local data that can guide sustainable CKD management and utilization strategies, contributing to reduced waste and environmental impact in cement production.

Keywords: cement kiln dust, CKD, cement bypass dust, CBD.

INTRODUCTION

Cement production plays a pivotal role in the global construction sector, with the demand for cement expected to reach 8.2 billion tons by 2030 according to World Cement Association [1]. Despite its economic and technological importance, cement production is associated with significant environmental challenges. Cement production is a significant contributor to global CO_2 emissions, responsible for about 8 % of the total emissions, which is approximately 2.8 billion tons of CO_2 in 2023 [2, 3]. Modern approaches to reduce CO_2 emissions in cement plants focus on optimizing energy efficiency through advanced kiln technologies and renewable energy integration, promoting circular economy practices such as: (i) material recycling and utilization of alternative raw materials as raw feed to reduce the consumption of limestone; (ii) indirect production of blended cements by partly replacement of Portland cement with alternative cementitious materials like fly ash and slag [4]. These strategies aim to transition towards a circular economy in cement production, minimizing waste and maximizing resource efficiency across the lifecycle of cement and concrete products [5]. The cement production is accompanied by generation of fine dust, known as cement kiln dust (CKD). CKD

is generated during the high-temperature processing of raw materials in the rotary kilns, where the temperature can exceed 1450°C [6]. The dust is transported in a stream of gas flowing from the burner throughout the rotary kiln and cyclone preheaters, after which is collected in bag filters or other bypass system. The CKD comprises a complex mixture of raw material and fuel residues, clinker dust, along with trace metals such as lead, chromium, and cadmium [7]. The composition of CKD is critical for understanding its potential impacts and applications. Typical CKD contains about 60 - 70 % calcium oxide (CaO), 15 - 20 % silicon dioxide (SiO_2), 5 - 10 % aluminum oxide (Al_2O_3), alkalis, chlorides, sulfates and varying amounts of other oxides and compounds [8, 9]. The composition of CKD varies significantly based on raw materials, specific kiln operation conditions and type of fuel [10]. The growing use of alternative fuels has necessitated significant modifications to production system and sometimes require additional dust removal methods. Often significant amount of chlorine is introduced to kiln with the usage of alternative fuels such as refuse-derived fuel (RDF) [11], municipal solid waste [12]; tyre-derived fuel (TDF) [13], biomass [14], etc. The alkali chlorides volatize and tend to accumulate as aggregates on the wall of the cyclone preheaters thus hindering their operational performance. For this reason, in modern cement plants bypass installation is applied between kiln and preheaters [15]. The dust from bypass removal system often is called cement bypass dust (CBD or CBPD). Cement kiln dust and cement bypass dust are often used as synonyms, but usually CBD is enriched in chlorine and potassium [9]. At the presented study the term cement kiln dust includes also the cement bypass dust.

All cement kilns generate CKD, where the quantities of the produced CKD depend on operational factors and the inputs to the manufacturing process [16]. Globally, the generation of cement kiln dust (CKD) is estimated to be between up to 20 % of the total cement production. Of course, collected CKD is re-used within the cement plants as raw feed material, but because of high alkali, sulfate and chloride content there is technological limits of re-using CKD, thus about 1/3 of the produced CKD is considered as industrial waste [10]. Since global cement production exceeds 4 billion metric tons annually, this suggests hundreds of millions of metric tons of CKD generated each year [10]. Furthermore, CKD has been successfully incorporated as a supplementary mineral additive in cement and concrete production, where it can partially replace clinker, reducing greenhouse gas emissions [17, 18]. The later application is limited due to the content of certain substances such as: alkali content which influence the settling time of the cement and may react chemically with certain aggregates (Alkali silicate reaction) in concrete mixtures; sulfates/chloride ions which promote steel corrosion in reinforced concrete. Moreover, there are strict requirements for sulfates (as SO_3) ≤ 4.0 % and chlorides ≤ 0.10 % in Portland cement, according to EN 197-1. Thus, utilization of CKD in cement and conventional concrete is limited. Additionally, CKD has been utilized in: neutralization of acidic waste streams and the immobilization of heavy metals in contaminated soils [19]; in soil stabilization projects to improve soil strength and reduce swelling in expansive soils [20], waste water treatment [21, 22], bricks production [23]. The non-utilized CKD brings environmental challenges. The leaching of heavy metals from CKD into groundwater is a major concern, necessitating proper management and treatment [10]. However, CKD's high content of calcium and other reactive components makes it a promising candidate for various beneficial uses.

Characterizing CKD from Bulgarian cement plants is essential for understanding its specific properties and exploring their potential applications at local scale. To the best of our knowledge studies about chemical and physical properties of Bulgarian CKD were not published digitally, yet. The present study aims to characterize CKD from three Bulgarian cement plants, focusing on the chemical and physical properties related to utilization of CKD in cementitious materials. The data obtained from this research are expected to contribute to sustainable cement production practices by providing local data and insights that support the development of effective CKD utilization strategies.

EXPERIMENTAL

Samples of cement kiln dust were provided from three local Bulgarian cement producing plants, hereinafter designated as CKD1, CKD2, and CKD3, correspondingly. The sample CKD1 was provided by a cement plant collected between cyclone preheaters and rotary kiln. The samples CKD2 and CKD3 were

provided by cement plants equipped with chlorine bypass dust collecting system, classifying them technically as cement bypass dust. All samples received were stored at airtight container to prevent hydration and carbonization from the atmospheric air.

Powder XRD analysis on the CKD samples was performed on Empyrean Powder X-ray diffractometer (Malvern Panalytical, Netherlands) in the 3°-100° 2θ range, overall scanning time 35 min, using Cu radiation at 40 kV and 30 mA and PIXcel3D detector. Initial phase identification was carried out using the HighScore Plus program [24]. The Rietveld refinement procedures have been carried out with the GSAS program and EXPGUI. Neutral atomic scattering factors, as these are stored in GSAS, have been used for all atoms [25, 26]. Infrared spectra of samples of 2 mg each as 13 mm in diameter KBr pressed pellets were recorded with a FT-IR spectrometer JASCO 4X (Japan) in the middle infrared spectral range between 4000 and 400 cm^{-1}, with a resolution of 4 cm^{-1} and 64 scans. Particle size distribution was evaluated by Mastersizer 3000 Malvern-Panalytical in dry dispersion mode. Chemical composition was determined using wave dispersive X-ray fluorescence (XRF) apparatus Rigaku Supermini 200 at 50 kV and 4 mA, with detecting elemental limits from F to U. Scanning electron microscopy (SEM) examinations of the CKD samples were performed on a ZEISS SEM EVO 25LS at a 15 kV acceleration voltage using two imaging regimes: in backscattered electrons (BSE) - for composition contrast and in secondary electrons (SE) - for topography contrast. The sample preparation included fixation of the powder material of each sample onto SEM stub using conducting carbon adhesive and then coating with carbon.

RESULTS AND DISCUSSION

Physical properties

The results from hygroscopicity, bulk and absolute density measurements showed similar physical properties of CKD2 and CKD3 (Table 1). The CKD1 showed lower bulk density, higher absolute density and lower hygroscopicity compared to others sample. The CKD's bulk and absolute densities are significantly lower compared to ordinary Portland cement which usually ranges from 0.83~1.6 g cm^{-3} for bulk density and 3.10 to 3.25 g cm^{-3} for absolute density. The measured hygroscopicity is relatively high, requiring special measures to prevent CKD from absorbing moisture from the atmosphere which initiate processes of hydration and carbonation.

Table 1. Bulk density, absolute density and hygroscopicity of cement kiln dust from three local cement plants.

Series	Bulk density, g cm^{-3}	Absolute density, g cm^{-3}	Hygroscopicity, %
CKD1	0.58	2.66	33.1
CKD2	0.66	2.46	71.3
CKD3	0.61	2.40	70.1

Particle size distribution

The samples are characterized by lognormal distribution of the curves with a pronounced bimodality (Fig. 1). The particle size of CKD3 is characterized by the finest particles, respectively by the highest specific surface area, followed by CKD2 and CKD1, with Brouckere mean diameters (D[4,3]) of 34 μm, 37 and 53 μm, respectively (Table 2). The 90 % of the total volume of the particles are below 80 μm, 102 μm and 136 μm for CKD3, CKD and CKD1.

Chemical composition of CKD

The results of the X-ray fluorescence analysis of the samples from the cement kilns dust of the three plants (Table 3) reveal similar composition for CKD2 and CKD3. The CKD1 showed highest content of CaO, SiO_2 and Al_2O_3. All samples contain significant contents of K_2O and Cl, where at samples CKD2 and CKD3 the amount reach 17 - 19 % for K_2O and 12 % for Cl. High chlorine content is common when alternative fuels were used (such as RDF) [9]. Other oxide compounds such as Fe_2O_3 from 1.5 to 2.7 %, MnO and ZnO < 1 % were found in the studied samples, most likely due to their presence in the raw material. The highest Fe_2O_3 content was measured at CKD1, which corresponds to the higher absolute density, registered for this sample. Trace amounts of Pb, ZnO, CuO and Br were detected (< 1 %) which need to be considered as potential environmental issues. The presence of bromine could be due to the use of RDF and/or electronic waste as fuel [27].

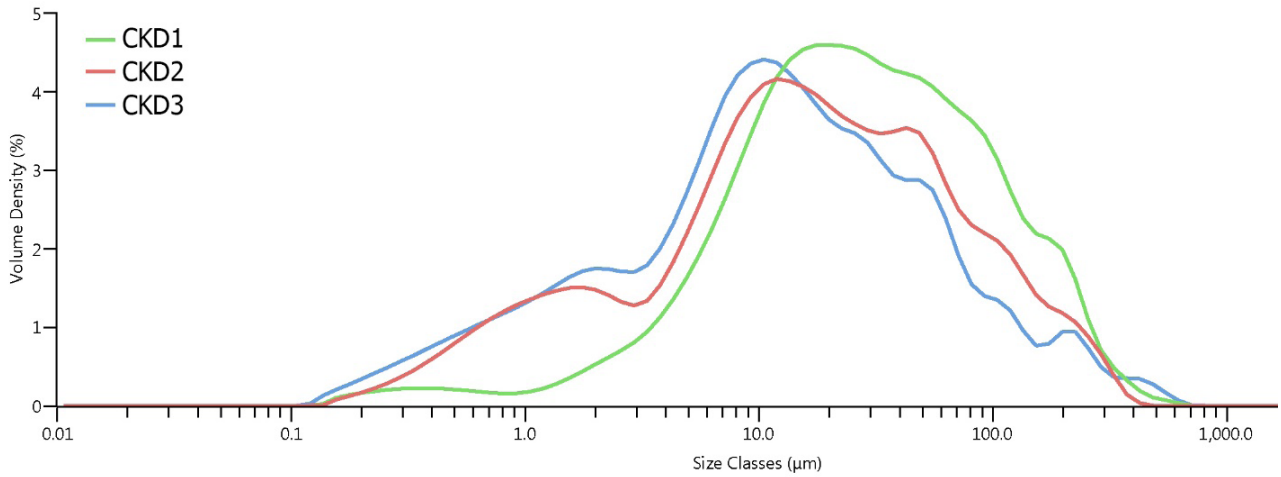

Fig. 1. Mie-sizing of powdered samples in dry air of cement kiln dust samples from the three plants.

Table 2. Particle size distribution parameters of cement kiln dust samples from the different plants.

Sample	D [3;2], µm	D [4;3], µm	Dv 10, µm	Dv 50, µm	Dv 90, µm	Specific surface area, $m^2 kg^{-1}$
CKD1	7.31	52.5	5.25	27	136	335.2
CKD2	3.61	37.4	1.28	15.6	102	678.6
CKD3	2.83	33.8	1.09	11.9	80.2	865.3

Table 3. Chemical composition of cement kiln dust samples from different cement plants, wt. %.

Oxide/ element	CKD1	CKD2	CKD3
Na_2O	0.14	1.51	1.79
MgO	0.60	0.47	0.50
Al_2O_3	2.81	1.79	1.93
SiO_2	12.37	5.39	5.47
P_2O_5	0.10	0.07	0.08
SO_3	0.88	4.39	5.96
Cl	3.70	11.81	11.70
K_2O	9.84	16.65	18.64
CaO	65.84	55.51	51.85
TiO_2	0.00	0.17	0.12
MnO	0.00	0.03	0.13
Fe_2O_3	2.70	1.59	1.42
CuO	0.03	0.06	0.02
ZnO	0.49	0.06	0.12
Br	0.04	0.16	0.08
PbO	0.45	0.34	0.19

Mineral phase composition of CKD

The main mineral phases in all three samples are lime, larnite and sylvite in different proportions (Fig. 2). The calcium contained in the examined CKDs is present in two main phases - free lime (CaO) and larnite ($Ca_2(SiO_4)$). The free lime is significantly lower in sample CKD1 compared to other samples. Part of the lime in the three samples has started to hydrate to portlandite ($Ca(OH)_2$) probably due to storage in contact with humidity. Spur rite phase ($Ca_5(SiO_4)_2(CO_3)$) was detected only in sample CKD1 and was probably formed in cement kiln as an early-formed reaction product of the raw precursors in the presence of Cl^- acting as mineralizer [28].

Sylvite content is significant (~ 20 - 21 %) in samples CKD2 and CKD3, and it is lower in CKD1, which correlates well with the chemical compositions presented in Table 3 and with measured hygroscopicity (Table 1). Sylvite, aphthitalite and other chlorides and sulphates are phases which was formed because of condensation from gaseous phase on raw material grains [29]. The aphthitalite phase (exceeding 12 wt%) was observed only in CKD3. This corresponds to the increased amount of potassium and sulphate in this sample as compared

to the other two. The aphthitalite is alkali sulphate considered here as a protogenetic phase, which differs from other sulphate phases originating from added calcium sulphates introduced to control the setting time of the Portland cement clinker [30]. The presence of alkali sulphates in cementitious systems could activate the pozzolanic reaction with fly ash or another reactive mineral additive [31].

The larnite (known also as belite - $Ca_2(SiO_4)$ or β-C_2S) phase amount, is higher in sample CKD1. The contents of Al_2O_3 and Fe_2O_3 are similar for all three cases and a certain positive correlation is observed between them (Table 3). This implies the entry of these metals into the composition of larnite as impurities, in which case their valences are possibly complemented to obtain an electroneutral structure, for example according to the scheme: $Si^{4+}+Ca^{2+} \leftrightarrow Al^{3+}+Fe^{3+}$. Small amounts of Cu, Zn, Mn, etc. probably also accumulate in the larnites as evidenced by the results of the XRF analyses (Table 3).

SEM images of CKD

The SEM examination (Fig. 3) reveals that the distribution and nature of the particles and aggregates exhibit similarities and differences in all three CKD materials. BSE images (Fig. 3a, c, e) of CKDs well highlight their distinctive features in both composition and microstructure. Sylvite (KCl) (brightest crystals in BSE images) is very well distinguished in CKD2 and CKD3 samples, and only sporadically occurs in SKD1. These data are in full agreement with the results of chemical and analysis, showing the lowest chlorine contents in the (CKD1), confirmed also by XRD analysis. Among all the crystalline phases in the studied CKD materials identified by XRD, sylvite forms the largest crystals, with sizes ranging from 10 - 35 μm (predominantly 20 - 35 μm) for CKD1, 10 - 30 μm (predominantly 15 - 20 μm) for CKD2, and 15 - 40 μm (predominantly 30 - 35 μm) for CKD3. The crystal sizes of all other crystalline phases are micron and submicron (Fig. 3b, d, f). Moreover, all CKD materials mainly consist of aggregates of micron and submicron polyphase particles. These aggregates vary in size, shape and cohesiveness. The aggregates sizes vary between first up to 300 μm. Conditionally according to their size, the aggregates can be divided into large (100 - 300 μm), medium (50 - 100 μm), small (20 - 50 μm) and very (small < 20 μm). In all samples, small and very small

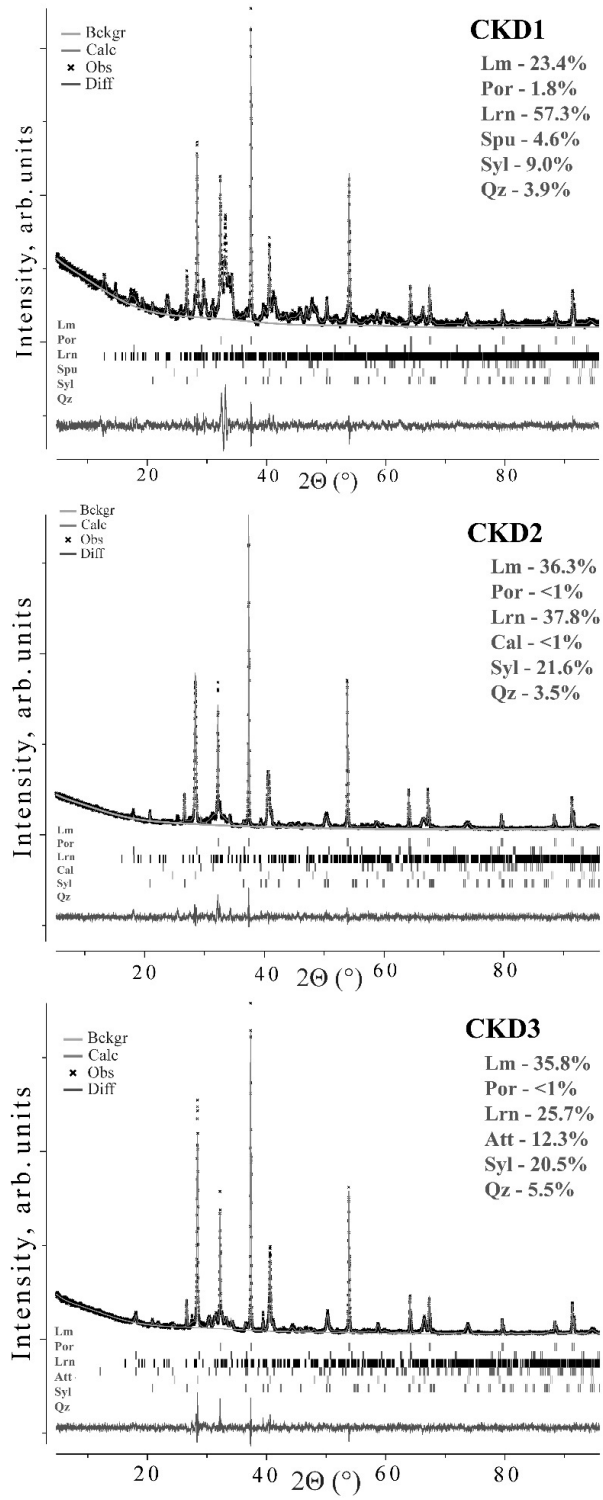

Fig. 2. Quantitative powder X-ray analysis (in wt. %) of cement kiln dust (CKD) from three local cement plants. Legend: lime CaO (Lm); portlandite $Ca(OH)_2$ (Por); larnite (belite) $Ca_2(SiO_4)$, β-C_2S, belite (Lrn); aphthitalite $K_3Na(SO_4)_2$ (Att); sylvite KCl (Syl); quartz SiO_2 (Qz); spurrite $Ca_5(SiO_4)_2.(CO_3)$ (Spu).

aggregates predominate. Large aggregates are more typical for CKD1 and CKD2, large and middle - for CKD3 (Fig. 3a, c, e).

FT-IR

The infrared spectra of analyzed cement kiln dusts (CKD1, CKD2 and CKD3) are graphically presented in Fig. 4. The analysis of the spectra and assignments of bands have revealed that the main constituents in the three samples are silica and calcium carbonate in the form of aragonite, which is in good agreement with the XRF and XRD analysis. There is certain indication for the presence of calcium oxide and hydroxide. The presence of silica and hydroxides is most distinctly

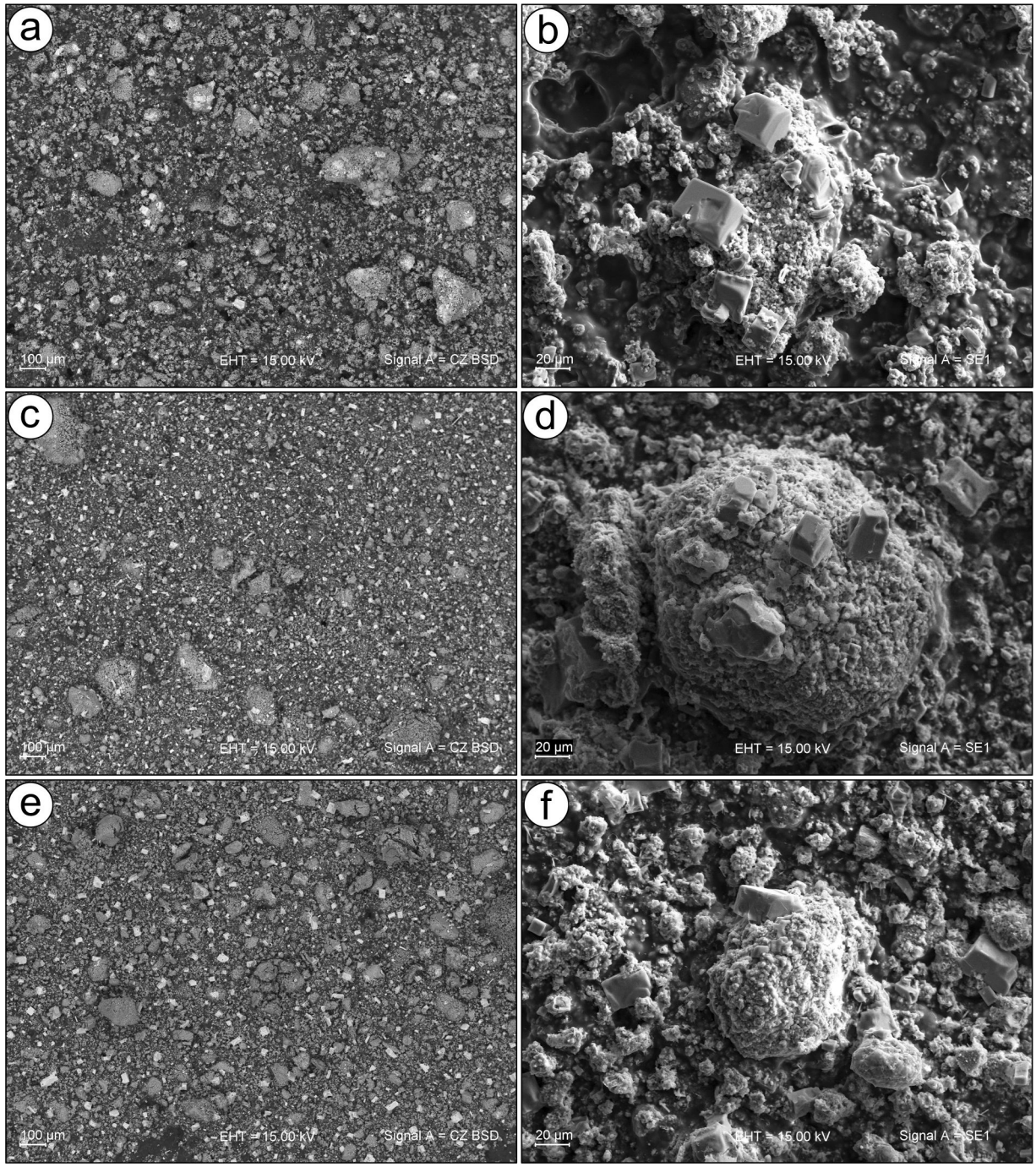

Fig. 3. SEM images of CKD: (a, b) - CKD1; (c, d) - CKD2; (e, f) - CKD3, images a, c and e - in BSE (the brightest particles in all CKDs are sylvite crystals); images b, d and f - in SE (sylvite crystals and polyphase aggregates in CKDs).

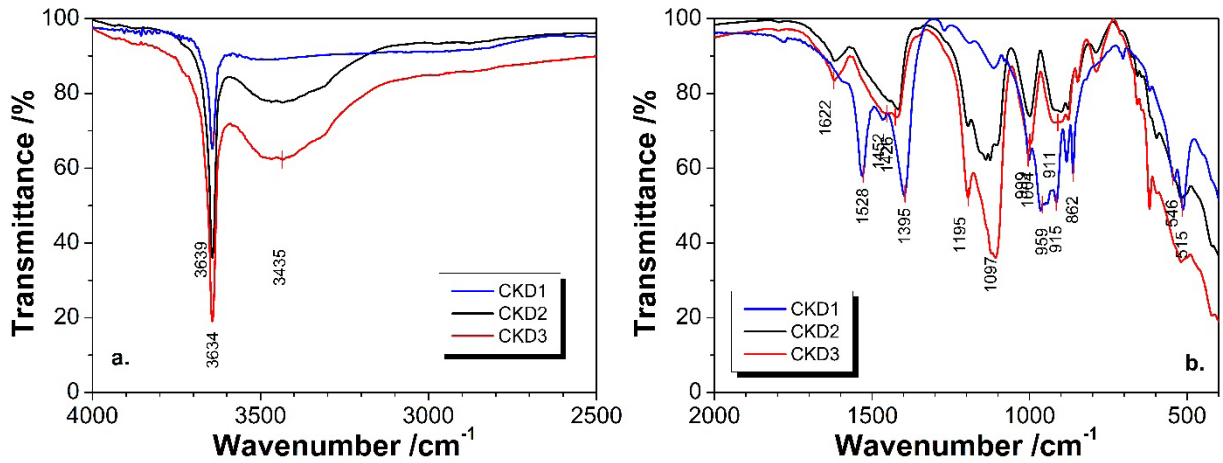

Fig. 4. Infrared spectra of the studied CKD samples: (a) Functional group region; (b) Fingerprint region.

revealed in the spectrum of CKD3, whereas in the spectrum of CKD1 it is least indicated. CKD3 contains higher amounts of calcium oxide and carbonates. CKD2 and CKD3 possess higher common similarity than compared to CKD1. The identified species are listed in Table 4.

CONCLUSIONS

The present study characterizes cement kiln dust (CKD) from three local cement plants, revealing variations in the physical, chemical, and mineralogical properties most probably being due to differences in the used raw materials, kiln conditions and usage of alternative fuels. The CKD2 and CKD3 showed very similar characteristics, whereas CKD1 differs in chemical and phase composition. The conclusions are summarised as:

- The CKD's bulk and absolute densities vary between 0.58 to 0.66 g cm^{-3} and 2.40-2.66 g cm^{-3}.
- The measured hygroscopicity are relatively high (up to 71 %) which require special measures to prevent CKD from absorbing moisture from the atmosphere.
- The chemical composition is characterized primarily by CaO. The K_2O content is significant reaching 19 %, and that one of Cl - up to 12 %. Trace amounts of Pb, ZnO, CuO and Br have been detected (< 1 %) which should be considered as potential environmental issues.

Table 4. IR frequencies of normal vibrations of identified species of cement kiln dust samples.

Species	Band measured, ν_m, cm^{-1}	Band reference, ν_r, cm^{-1}
OH-group	3639, 3634	3644 [32]
Si-OH	3434	3425 [33]
$CaCO_3$ (aragonite)	1528	1504[34]
C=O (carbonate)	1395	1420[32]
Si-O-Si	1097	1087 [32], 1040 [35]
CaO	861	875 [32]

- The mineral composition of the analysed CKD comprises mostly of lime (23 - 37 %), larnite (26 - 57 %), sylvite (9 - 22 %), and quartz (4 - 6 %). Other phases such as: aphthitalite (12 % in CKD3), spur rite (5 % in CKD1), portlandite (< 2 %) and calcite < 1 % were also detected.
- SEM examination has revealed that CKD samples have differences in particle and aggregate distribution, with sylvite crystals being most prominent in CKD2 and CKD3 however sporadic in CKD1. The aggregates in all samples predominantly consist of small and very small polyphase particles, with larger aggregates more common in CKD1 and CKD2.

Acknowledgements

The results in this work have been achieved in fulfilment of a project financed by the National Science Fund of Bulgaria under contract No. КП-06-Н77/9 from 4.12.2023.

***Authors' contributions**: Conceptualization: A. N.; XRD: V. K.; SEM: M. T.; XRF: L. T.; FT-IR: N. J.; Absolute density: E. K.; Sampling: A. N., I. R.; Data curation, writing: all authors.*

REFERENCES

1. N. Tkachenko, K. Tang, M. McCarten, S. Reece, D. Kampmann, C. Hickey, M. Bayaraa, P. Foster, C. Layman, C. Rossi, K. Scott, D. Yoken, C. Christiaen, B. Caldecott, Global database of cement production assets and upstream suppliers, Sci. Data, 10, 1, 2023, 696.
2. A.L. De la Colina Martínez, D.J. Delgado Hernández, Circular Cement Decarbonisation: Towards a Net-Zero Built Environment, in Environmental Engineering and Waste Management: Recent Trends and Perspectives, Springer, 2024, 269-296.
3. R.M. Andrew, Global CO_2 emissions from cement production, Earth Syst. Sci. Data, 10, 1, 2018, 195-217.
4. K.L. Scrivener, V.M. John, E.M. Gartner, Eco-efficient cements: Potential economically viable solutions for a low-CO_2 cement-based materials industry, Cem. Concr. Res., 114, 2018, 2-26.
5. A. Genovese, A. Acquaye, A. Figueroa, S.L. Koh, Sustainable supply chain management and the transition towards a circular economy: Evidence and some applications, Omega, 66, 2017, 344-357.
6. S. Ghosh, Advances in Cement Technology: Chemistry, Manufacture and Testing, Elsevier, 2003.
7. A.A. Elbaz, A.M. Aboulfotoh, A.M. Dohdoh, A.M. Wahba, Review of beneficial uses of cement kiln dust (CKD), fly ash (FA) and their mixture, J. Mater. Environ. Sci., 10, 11, 2019, 1062-1073.
8. O.S. Khanna, Characterization and utilization of cement kiln dusts (CKDs) as partial replacements of Portland cement, University of Toronto, 2009.
9. D. Barnat-Hunek, J. Gora, Z. Suchorab, G. Lagod, Cement kiln dust, in Waste and Supplementary Cementitious Materials in Concrete, Elsevier, 2018, 149-180.
10. A.Y. Al-Bakri, H.M. Ahmed, M.A. Hefni, Cement Kiln Dust (CKD): potential beneficial applications and eco-sustainable solutions, Sustainability, 14, 12, 2022, 7022.
11. I. Chamurova, R. Stanev, N. RDF as an alternative fuel for the cement plants in Bulgaria. J. Chem. Technol. Metall. 52.2, 2017, 355-361.
12. L. Wang, X. Huang, X. Li, X. Bi, D. Yan, W. Hu, J.R. Grace, Simulation of heavy metals behaviour during Co-processing of fly ash from municipal solid waste incineration with cement raw meal in a rotary kiln, Waste Manage., 144, 2022, 246-254.
13. M.J. Pegg, P.R. Amyotte, M. Fels, C.R. Cumming, J.C. Poushay, An assessment of the use of tires as an alternative fuel, Final Report, 2007.
14. J.M. Lobert, K.W. Keene, J. Logan, R. Yevich, Global chlorine emissions from biomass burning: Reactive Chlorine Emissions Inventory, J. Geophys. Res. Atmos., 104(D7), 1999, 8373-8389.
15. P. Czapik, J. Zapała-Sławeta, Z. Owsiak, P. Stepien, Hydration of cement by-pass dust, Constr. Build. Mater., 231, 2020, 117139.
16. U.S. Environmental Protection Agency (EPA), Report to Congress on cement kiln dust, 1993, EPA-530-R-94-001.
17. R. Siddique, Utilization of cement kiln dust (CKD) in cement mortar and concrete - an overview, Resour. Conserv. Recycl., 48, 4, 2006, 315-338.
18. A. Popov, G. Chernev. The effect of cement kiln dust on the properties of cement. J. Chem. Technol. Metall., 2024, 59.6, 1341-1346.
19. D.H. Moon, J.R. Lee, D.G. Grubb, J.H. Park, An assessment of Portland cement, cement kiln dust and Class C fly ash for the immobilization of Zn in contaminated soils, Environ. Earth Sci., 61, 2010, 1745-1750.
20. S. Gupta, M. Pandey, R. Srivastava, Evaluation of cement kiln dust stabilized heavy metals contaminated expansive soil-a laboratory study, Eur. J. Adv. Eng. Technol., 2, 6, 2015, 37-42.
21. M. El Zayat, Adsorption of heavy metals cations in wastewater using cement kiln dust, AUC Knowledge Fountain, 2015.
22. A.W. Taha, A.M. Dakroury, G.O. El-Sayed, S.A. El-Salam, Assessment removal of heavy metals ions from wastewater by cement kiln dust (CKD), J. Am. Sci., 6, 12, 2010, 910-917.

23. M.M. El-Attar, D.M. Sadek, A.M. Salah, Recycling of high volumes of cement kiln dust in bricks industry, J. Clean Prod., 143, 2017, 506-515.
24. T. Degen, M. Sadki, E. Bron, U. König, G. Nénert, The highscore suite, Powder Diffr., 29, S2, 2014, S13-S18.
25. A. Larsen, R. Von Dreele, General Structure Analysis System (GSAS), Report LAUR 86-748, Los Alamos National Laboratory, New Mexico, USA, 2000.
26. B.H. Toby, EXPGUI, a graphical user interface for GSAS, J. Appl. Crystallogr., 34, 2, 2001, 210-213.
27. A. Nikolov, L. Tsvetanova, B. Barbov, B. Ranguelov, M. Tarasov, E-waste as a potential precursor for geopolymers, IOP Conf. Ser. Mater. Sci. Eng., 1323, 1, 2024, 012004.
28. H. Bolio-Arceo, F. Glasser, Formation of spurrite, $Ca_5(SiO_4)_2CO_3$, Cem. Concr. Res., 20, 2, 1990, 301-307.
29. W. Kurdowski, Cement and Concrete Chemistry, Springer Science & Business, 2014.
30. Y. Ma, X. Li, J. Qian, X. Shen, Effect of protogenetic alkali sulfates on the hydration and hardening of cement with different tricalcium aluminate content, Constr. Build. Mater., 256, 2020, 119475.
31. Y. Ma, J. Qian, Effect of alkali sulfates in clinker on hydration and hardening properties of cement incorporating SCMs, Adv. Cem. Res., 35, 8, 2022, 345-357.
32. A.I. Hussein, Synthesis and characterization of spherical calcium carbonate nanoparticles derived from cockle shells, Appl. Sci., 10, 20, 2020, 7170.
33. D.M. Widjonarko, J. Jumina, I. Kartini, N. Nuryono, Phosphonate modified silica for adsorption of Co(II), Ni(II), Cu(II), and Zn(II), Indones. J. Chem., 14, 2, 2014, 143-151.
34. K. Nakamoto, Infrared and Raman spectra of inorganic and coordination compounds, part B: applications in coordination, organometallic, and bioinorganic chemistry, John Wiley & Sons, 2009.
35. E. Herth, R. Zeggari, J.Y. Rauch, F. Remy-Martin, W. Boireau, Investigation of amorphous SiOx layer on gold surface for Surface Plasmon Resonance measurements, Microelectron. Eng., 163, 2016, 43-48.